THE JOURNAL OF BIOLOGICAL CHEMISTRY VOL. 283, NO. 29, pp. 20243–20251, July 18, 2008

Transcription Termination Factor Rho Prefers Catalytically Active Elongation Complexes for Releasing RNA*

Received for publication, March 10, 2008, and in revised form, May 15, 2008 Published, JBC Papers in Press, May 15, 2008, DOI 10.1074/jbc.M801926200

Dipak Dutta, Jisha Chalissery[1], and Ranjan Sen[2]

From the Laboratory of Transcription Biology, Centre for DNA Fingerprinting and Diagnostics, ECIL Road, Nacharam, Hyderabad-500076, India

RNA polymerase pauses at different DNA sequences during transcription elongation, and this pausing is associated with distinct conformational state(s) of the elongation complex (EC). Transcription termination by the termination factor Rho, an RNA-dependent molecular motor, requires pausing of the EC in the termination zone of Rho-dependent terminators. We hypothesized that the conformational state(s) of the EC associated with this pausing would influence the action of Rho. Analyses of the pausing behavior of the EC at the termination points of two well known Rho-dependent terminators revealed that Rho prefers actively transcribing complexes for termination. RNA release kinetics from stalled ECs showed that the rate of RNA release by Rho was reduced if the EC was irreversibly backtracked, if its RNA exit channel was modified by an RNA hairpin, or the bridge helix/trigger loop movement in its active site was perturbed. These defects were overcome significantly by enhancing the rate of ATP hydrolysis either by increasing the concentration of ATP or by using a Rho mutant with higher ATPase activity. We propose that the force generated from ATP hydrolysis of Rho is the key factor in dislodging the EC through its molecular motor action, and this process is facilitated when the EC is in a catalytically competent state, undergoing rapid "Brownian ratchet" motion.

The highly processive and stable EC[3] (1–3) dissociates from template DNA only in response to transcription termination signals. There are two types of termination signals in *Escherichia coli*. The intrinsic terminators are characterized by a GC-rich inverted repeat followed by an oligo(dT) stretch that destabilizes the EC and the factor-dependent terminators, which depend on an essential protein, called Rho, for termination (4, 5).

Rho is a homo-hexameric RNA/DNA helicase or translocase capable of dissociating the elongating RNA polymerase from the template DNA by utilizing its RNA-dependent ATPase activity (6–8). It recognizes the Rho utilization (*rut*) site on the exiting mRNA through its N-terminal primary RNA binding domain (9). Binding of RNA to the primary binding site of Rho guides the 3′-side of the RNA into the central hole of the hexamer, which constitutes the secondary RNA binding domain. Q-loop and R-loop are the two major RNA binding determinants of Rho at this site. Interaction of the RNA with these two loops activates ATP hydrolysis in the nearby P-loop region (10–16).

The Rho-dependent termination region consists of a proximal 70–80-nt stretch of Cys-rich, unstructured RNA for binding of Rho (the *rut* site; see Refs. 17–19), followed by a distal termination zone, dispersed over a wide range, beginning about 60–90 nts downstream of the *rut* site (reviewed in Ref. 20). Analyses of Rho-dependent terminators revealed that the position of the *rut* site determines the location of the downstream termination zone (21–24). Unlike Rho-independent terminators, the termination zone of the well characterized Rho-dependent terminators, such as λ *tR1* and *trp t′*, do not have characteristic signatures, except that the sequences are AU-rich and the termination points are associated with pausing of the EC (25, 26). However, not all pause sites are termination points, and these include some of the strongest pauses along a terminator (27).

RNAP pauses during elongation at different sequences, which provide an adequate time window for different *cis* and *trans* factors to act upon the EC (28). Depending on the pause sequence, the active site of the EC can be in conformationally distinct states (28). Pausing at Rho-independent terminators is required for the timely formation of an RNA hairpin at the exit channel (29), although pausing in the termination zone of Rho-dependent terminators is believed to help Rho to "catch up" with the elongating EC (7).

The importance of conformational state(s) of the EC in Rho-dependent termination has not been explored. As pausing of the EC is associated with the termination points in the termination zone (25, 26), we hypothesized that the conformational state(s) associated with pausing would affect the RNA release process by Rho. Quantitative analyses of the EC paused at the termination points, and RNA release kinetics from the stalled ECs with different conformational states show that Rho prefers actively transcribing complexes for termination. These assays also reveal that an enhanced rate of ATP hydrolysis is required to release RNA from the catalytically inactive ECs. We propose that the force generated by ATP hydrolysis of Rho is the key factor in dislodging the EC through its molecular motor action,

* This work was supported by a Wellcome Trust Senior Research Fellowship (to R. S.) and funding from Department of Biotechnology, India. The costs of publication of this article were defrayed in part by the payment of page charges. This article must therefore be hereby marked "*advertisement*" in accordance with 18 U.S.C. Section 1734 solely to indicate this fact.

[1] University Grants Commission Senior Research Fellow.

[2] To whom correspondence should be addressed: Laboratory of Transcription Biology, Centre for DNA Fingerprinting and Diagnostics, ECIL Rd., Nacharam, Hyderabad-500076, India. Tel.: 91-40-27151344 (Ext. 1401); Fax: 91-40-27155610; E-mail: rsen@cdfd.org.in.

[3] The abbreviations used are: EC, elongation complex; RNAP, RNA polymerase; WT, wild type; IPTG, isopropyl 1-thio-β-D-galactopyranoside; RB, road-blocked complex; BH, bridge helix; TL, trigger-loop; STL, streptolydigin; TGT, tagetitoxin.

TABLE 1
Oligos and plasmids used in this study

	Description
Oligo	
RS58	ATAAACTGCCAGGAATTGGGGATC; located upstream of *T7A1* promoter of pRS106
RS83	ATAAACTGCCAGGAATTGGGGATC; 5′-biotinylated RS58
RS139	TTAATACGACTCACTATAGGGAGATCGAGAGGGACACGGGCG. T7 ϕ-10 promoter fused to the start site of *T7A1* promoter
RS140	GTCCGGATTGGAGCTTGGGATCC; reverse oligo at BamHI site of pRS106
RS146	GCGCGCAAGCTTGCGATCAACAAGGCCATTCATGC, λ *t*R1 forward primer with HindIII site
RS147	GCGCGCGGATCCCCCCATTCAAGAACAGCAAGCAGC, reverse oligo to generate T7A1-λ *t*R1 terminator template
RS177	TTGTGAGCGCTCACAATTCGGATATATATTAACAATTACCTG; reverse oligo with *lac* operator sequence, used to generate roadblock downstream of rut sites of T7A1-*trp t′* template
RS270	GCGCGCCATATGAAAACGCCCCTGGTTACCCG, forward primer with NdeI site to amplify *E. coli greB* gene
RS272	GCGCGC*CTCGAG*CGGTTTCACGTACTCGATAGCATTAAC, reverse primer with XhoI site, without stop codon, to amplify *E. coli greB*
RS275	GGAATTGTGAGCGCTCACAATTCCTTC*CA*GCACACATCGCCTGAAAGACTAG; reverse oligo with *lac* operator sequence 4 nt downstream of the *his* pause position, used for PCR amplification with RS83/RS307 on *his* pause template
RS302	GAATTGTGAGCGCTCACAATTCTTAGGAAAATTATTGATTTACTG; reverse oligo with *lac* operator sequence; used to generate roadblock downstream of *T7A1* promoter
RS307	AGCACACATCGCCTGAAAGACTAGTCAGGATGATGGTGATATATTAACAATTACCTG; reverse oligo with *his* pause sequence; specific for T7A1-*trp t′* template
RS314	AGTGACTTAGAGAAAAAAGCACGCTACCGCCTGGCCTAGGTGTTATGTTGCGGGATT; reverse primer with *ops* pause sequence from *rfa*Q gene; used downstream of *T7A1* promoter
RS315	GGAATTGTGAGCGCTCACAATTCAAGCACGCTACCGCCTGGCCTA; reverse oligo with *lac* operator fusion 4 nt downstream of *ops* pause site; used on RS83/RS314 template
RS319	AGTGACTTAGAGAAAAAAGCACGCTACCGCCGAGGAATAAGTGACTTAGAG; reverse oligo with *lac* operator sequence, used to generate roadblock downstream of *T7A1* promoter and rut sites
RS320	GGAATTGTGAGCGCTCACAATTCAAGCACGCTACCGCCGAGGAATAAGTGACTTAGAG; reverse oligo with *lac* operator fusion 4 nt downstream of ops pause site; used with RS83/RS319 template
RS341	GAA TTG TGA GCG CTC ACA ATT C GGATCCTTAGATAACAATTGATTGAATG; 67 nt downstream of λ nutR site
RS345	GCTTCTACCTTTGACGAACACGCATCTCGCCACGTTC, primer 1 for site-directed mutagenesis to make P235H Rho
RS346	GAACGTGGCGAGATGCGTGTTCGTCAAAGGTAGAAGC, primer 2 for site-directed mutagenesis to make P235H Rho
Plasmids	
pRS22	See Ref. 30
pRS96	See Ref. 31
pRS103	λ *t*R1 fragment cloned at HindIII/BamHI site of pRS22
pRS106	See Ref. 50
pRS604	T7A1-λ *t*R1 fragment cloned at HindIII site of pRS22
pRS630	P235H Rho cloned at XhoI/NdeI site of pET 21b, His-tagged at C terminus

and the process is facilitated when the EC is in a catalytically competent state undergoing rapid "Brownian ratchet" motion.

EXPERIMENTAL PROCEDURES

Materials—NTPs, poly(C), IPTG, lysozyme, dithiothreitol, and bovine serum albumin were from GE Healthcare. Radioisotopes [γ-^{32}P]ATP (6000 Ci/mmol) and [α-^{32}P]CTP (4500 Ci/mmol) were purchased from either GE Healthcare or Jonaki, BRIT, India. Primers for PCR were obtained either from Sigma or MWG Biotec. Restriction endonucleases and T4 DNA ligase were from New England Biolabs. WT *E. coli* RNA polymerase holoenzyme and tagetitoxin were purchased from Epicenter Biotechnologies. *Taq*DNA polymerase was from Roche Applied Science. Streptavidin-coated magnetic beads were from Pierce. Streptolydigin was from Chemcon, Germany.

Cloning, Overexpression, and Purification of Proteins—The purification of LacR, NusA, NusG, His-tagged and nonHis-tagged Rho was performed as described previously (30, 31). His-tagged *E. coli* GreB was cloned in pET21b and purified using nickel-nitrilotriacetic acid beads. P235H Rho (pRS630) was prepared by site-directed mutagenesis (Stratagene) of pRS96, using the primers RS345 and RS346, and was purified as described earlier (31).

Templates for in Vitro Transcription—T7A1-*trp t′* and T7A1-λ *tR1* templates for pausing assays, used in Fig. 1, were made by PCR amplification using RS58/RS140 primers with the plasmid pRS106 (31) and RS58/RS147 primers with plasmid pRS604, respectively. To immobilize the templates on streptavidin-coated magnetic beads (Promega), a biotinylated upstream primer RS83 was used in all cases. Primers with *lac* operator, *ops* pause, and *his* pause sequences were used in PCRs to incorporate these sequences in the termination zone of the *trp t′* terminator. Details of the primers and plasmids are described in Table 1.

Pausing Kinetics Assays—All *in vitro* transcription assays were performed in T buffer (25 mM Tris-HCl, pH 8.0, 5 mM $MgCl_2$, 50 mM KCl, 1 mM dithiothreitol, and 0.1 mg/ml bovine serum albumin) at 37 °C. The reactions were initiated with 10 nM DNA template, 40 nM WT RNA polymerase, 175 μM ApU, 5 μM each of GTP and ATP, and 2.5 μM of CTP to make a 23-mer elongation complex (EC_{23}). [α-^{32}P]CTP (3000 Ci/mmol) was added to the reaction to label the EC_{23}. EC_{23} was then chased with 20 μM NTPs in the presence of 10 μg/ml rifampicin, and aliquots were removed at different time points and mixed with formamide loading dye (Fig. 1, *A* and *B*). Transcripts were fractionated by electrophoresis on a 10% sequencing gel, and the gels were scanned and analyzed by Typhoon 9200 PhosphorImager. Pausing assays on *ops* (Fig. 3*B*) and *his* (Fig. 4*B*) pause templates were performed essentially in the same way as described above, except that EC_{23} was chased with 10 μM GTP and 100 μM other NTPs.

Rho-mediated RNA Release Assays from Stalled Elongation Complexes (RB; Road-blocked Complex)—These assays were performed in T buffer using immobilized templates with *lac* operator sequences at different positions in the termination zone of the T7A1-*trp t′* template (Figs. 2–4). The templates were immobilized before starting the reaction. Transcription

reactions were initiated as above except that 100 nM of *lac* repressor was added before making the EC_{23} complex. EC_{23} complex was then chased in the presence of 100 μM NTPs and rifampicin for 2 min to make the RB complexes. RB complexes were made in a similar manner on all the templates. These complexes were then immediately washed three times with 150 μl of T buffer to remove the excess NTPs and resuspended in the same buffer. The washing steps were completed within 5 min to avoid long incubation of the stalled ECs. 50 nM Rho in the presence of indicated amounts of ATP (either 25 μM or 1 mM) was then added, and aliquots of the reaction mixture were removed at different time points, and supernatant and bead fractions were separated using a magnetic stand. Half of the supernatant ("S") was added to an equal volume of RNA loading dye (Ambion), and the rest of the reaction (half of the supernatant + pellet; "P") was phenol-extracted and mixed with the same dye. In the experiments where antibiotics were used, the RB complexes were incubated with either 300 μM streptolydigin or 60 μM tagetitoxin for 5 min before the addition of Rho.

GreB and Pyrophosphate Cleavage Assays—To assess the extent of backtracking of the stalled elongation complexes at position +124 (Fig. 2*B*) and at *ops* pause site (Fig. 3*B*), the respective RB complexes were prepared as described above. The backtracked complex at +124 was observed to form readily during the three washing steps, which were completed within 5 min. Then 0.5 μM of GreB was added, and the cleavage reactions were allowed to continue for 3 min. For pyrophosphate (PP_i)-mediated cleavage of the RB complex at the *his* pause site, 1 mM sodium pyrophosphate was added, and aliquots of the reaction mixture were removed at the indicated (Fig. 4*C*) time points, and the reaction was stopped by mixing with RNA loading dye.

Analyses of the Pausing and RNA Release Kinetics—For the pausing assays, the amount of RNA in each pausing site (Fig. 1) was quantitated using ImageQuant software and plotted against time. The plots were fitted to the equation of exponential decay ($y = a\ \exp^{-(\lambda t)}$) to calculate the rate (λ) of escape from the paused site and efficiency of pausing (a) at that site (stated as *PE* in Fig. 1). The intercept of this curve on the y axis gives the value of "$t_{1/2}$", the pausing efficiency. The half-lives ($t_{1/2}$) of pausing were calculated from, $t_{1/2} = \ln 2/(\lambda \ln 10)$.

To determine the rate of accumulation of Rho-mediated released RNA (Figs. 2–5), the band intensities were quantitated by ImageQuant software, and the fraction of released RNA (2S/S + (S + P)) from each experiment was plotted against time. The plots were fitted to the equation of exponential rise ($y = a(1 - \exp^{-\lambda t})$) to calculate the rate (λ) and maximum efficiency (a) of RNA release. The error bars were calculated from the standard deviations obtained from at least three measurements. All the curve fittings were performed using Sigmaplot.

ATPase Assays—The rate of ATP hydrolysis of WT Rho and Rho P235H was measured by using RNAs containing the region of well known Rho-dependent λ *tR1* and *trp t′* terminators. DNA templates for transcribing the RNA were prepared by PCR amplification from the plasmid pRS604 using RS139/RS341 oligo pairs, and from the plasmid pRS106 using RS139/RS177 oligo pairs, to make the λ *tR1* and *trp t′* terminator sequence containing RNA fragments, respectively (Table 1). Both the RNAs were made using the Mega transcript kit from Ambion. The ATP hydrolysis was assayed by monitoring the release of P_i from ATP using polyethyleneimine TLC plates and 0.75 M KH_2PO_4, pH 3.5, as a mobile phase under the following conditions. The assays were performed in T buffer (25 mM Tris-HCl, pH 8.0, 50 mM KCl, 5 mM $MgCl_2$, 1 mM dithiothreitol, 0.1 mg/ml bovine serum albumin) at 37 °C. The rate of ATP hydrolysis at 25 μM and 1 mM of ATP together with [γ-^{32}P]ATP (3500 Ci/mmol; BRIT, India) were measured using 25 nM and 50 nM of Rho, respectively. Reaction was started by addition of 0.2 μM of either λ *tR1* or *trp t′* RNA. Aliquots were removed and stopped with 1.5 M formic acid at various time points depending on the concentrations of ATP. Release of P_i was analyzed by exposing the TLC sheets to a PhosphorImager screen and subsequently by scanning using Typhoon 9200 (Amersham Biosciences) and quantified by ImageQuant TL software. The product formation was linear in the time range that we used for calculating the initial rate of the reaction. The initial rates of the reaction were determined by plotting the amount of P_i released *versus* time using linear regression methods.

RESULTS

Pausing of ECs at the Termination Points of Rho-dependent Terminators Is Associated with a Short Half-life—Earlier semi-quantitative studies with two well known Rho-dependent terminators, *trp t′* and λ *tR1* (24, 25), described the pausing of RNAP at the termination points in the termination zone of these two terminators. To further characterize the nature of these pauses, we cloned these two terminators under a strong promoter like *T7A1*, and we measured pausing kinetics at the major termination points (indicated by * in Fig. 1, *A* and *B*). Band intensities corresponding to the pausing sites were plotted against time and fitted to an exponential decay equation to calculate the pause half-lives ($t_{1/2}$) and pause efficiencies (Fig. 1, shown below the *autoradiograms*). We observed that at all the termination points, except at position 124 of *trp t′*, the half-lives of pausing are very short. This suggests that the nucleotide addition cycle at these points is not hindered significantly, and the ECs are in a catalytically active state. Even though the EC pauses longer at position 124 of *trp t′* than the other pausing sites, it retains the competence for elongation at this point. We also observed that the pausing efficiencies at the termination points of the λ *tR1* terminator are higher than that of *trp t′* terminator. It should be noted that the difference in the RNA sequences between the two terminators may also lead to the difference in the ability of the Rho to act.

We concluded that although high efficiency pausing in the termination zone is important for termination to occur, Rho distinctly prefers catalytically active conformational states of the EC. Transient pauses are preferred over long pauses for releasing RNA by Rho.

Rationale and Design of RNA Release Assays from Stalled ECs—To gain further insight into the preference of Rho for particular conformational state(s) of the EC, we measured the rates and efficiencies of RNA release by Rho from ECs in different conformational states. We stalled elongation complexes

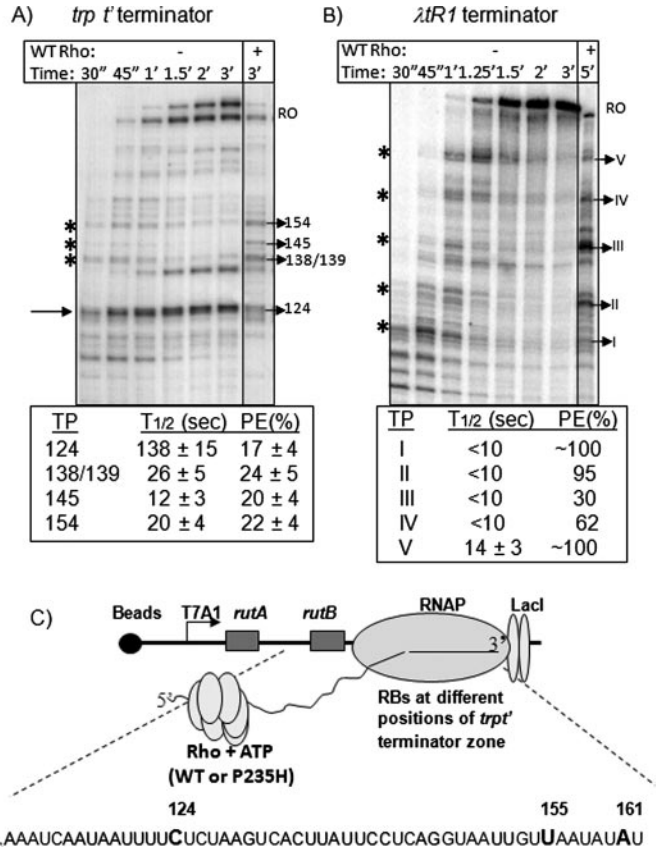

FIGURE 1. **Analyses of pausing associated with the Rho-dependent termination points in trp *t'* and λT_{R1} terminators.** Autoradiograms show the elongation kinetics through the termination zones of *trp t'* (*A*) and λ *tR1* terminators (*B*). *Right-most lane* of each of the autoradiograms shows the terminated RNA bands in the presence of Rho. The *numbering* next to the autoradiogram in *A* denotes the positions of the terminated band with respect to the transcription start site. The numberings (*I–V*) in autoradiogram *B* are the positions of the terminated bands in the λ *tR1* terminator. *Asterisk* indicates the paused bands corresponding to the positions of termination. *Below* each autoradiogram the pause half-lives ($t_{1/2}$) and pausing efficiencies (*PE*) corresponding to each termination point (*TP*) are shown. *RO* denotes run-off transcript. *C,* schematic showing the design of the stalled elongation complex (*RB*) at different positions of the *trp t'* terminator zone. The DNA template consists of a *T7A1* promoter followed by *rutA* and *rutB* sites and the termination zone of *trp t'* terminator. The *lac* operator sequence was introduced at different positions to stall the elongation complex in the presence of the *lac* repressor. The sequence of the termination zone is described below the schematic. To these different RBs either WT or P235H Rho were added to initiate RNA release reactions.

(RB) at desired positions in the termination zone of the *trp t'* terminator using *lac* repressor as a roadblock (Fig. 1*C*) (32) so that the behavior of Rho could be studied uncoupled from transcription elongation. We prepared four different types of stalled ECs as follows: 1) catalytically active EC at position +161 (Fig. 2); 2) an irreversibly backtracked EC at position +124 (Fig. 2); 3) a reversibly backtracked EC at *ops* pause site introduced at position +155 (Fig. 3) (33); and 4) catalytically inactive EC stalled at *his* pause site at position +199 with an RNA hairpin at the RNA exit channel (Fig. 4) (33–36). We also prepared stalled ECs at position +161 with conformationally frozen active centers using two antibiotics, tagetitoxin (37) and streptolydigin (38, 39). All these stalled ECs were made on immobilized DNA templates attached to magnetic beads, which facilitated the removal of NTPs after formation of the complexes. RNA release by Rho was initiated in the presence of ATP.

TABLE 2
ATPase activity under different conditions

The errors were calculated from 3 to 4 independent measurements. The fold increase in the rate of ATP hydrolysis under different conditions was expressed with respect to that obtained with the WT Rho in the presence of 0.025 mM ATP.

Rho	[ATP]	Rate of ATP hydrolysis	Fold increase
	mM	*nmol/min/μg Rho*	
A. λ *tR1* RNA			
WT	0.025	0.22 ± 0.03	(1)
WT	1.0	1.49 ± 0.08	6.7
P235H	0.025	0.86 ± 0.08	3.9
P235H	1.0	4.58 ± 0.57	20.8
B. *trp t'* RNA			
WT	0.025	0.16 ± 0.03	(1)
WT	1.0	1.51 ± 0.17	9.4
P235H	0.025	0.87 ± 0.01	5.4
P235H	1.0	5.95 ± 0.44	37.2

RNA-dependent ATPase activity of Rho is required for its transcription termination activity (40, 41). We hypothesized that change in the rate of ATP hydrolysis may have a direct consequence on the rate of RNA release by Rho from the stalled ECs. The ATP hydrolysis rate may be varied by changing the ATP concentration or by using certain Rho mutant(s) with significantly different ATPase activity. We measured the rate of ATP hydrolysis on two RNA fragments containing the λ *tR1* and *trp t'* terminator sequences under different conditions (Table 2, A and B). Upon increasing the concentration of ATP from 25 μM to 1 mM, the rate of ATP hydrolysis increased to ~7-fold for λ *tR1* and ~9-fold for *trp t'* RNA. We used a Rho mutant, P235H, reported to have a higher rate of ATP hydrolysis compared with WT (42). Consistent with this report, we observed that in the presence of 25 μM of ATP, the rate of ATP hydrolysis of this mutant is ~4-fold higher for λ *tR1* and ~5-fold higher for *trp t'* RNA compared with that observed for WT Rho. Therefore, to elucidate the effect of rate of ATP hydrolysis on the rate of RNA release by Rho, we compared the RNA release kinetics from the stalled ECs under conditions of low (25 μM ATP) and high (1 mM ATP/P235H Rho) rates of ATP hydrolysis.

It is believed that the free energy generated during the ATP hydrolysis is required for the translocation of Rho along the RNA (43). Therefore, it can be assumed that the translocation speed along the RNA is proportional to the rate of ATP hydrolysis. As the translocation speed of Rho remains the same in the presence of a given concentration of ATP, the release kinetics obtained from our experiments will be the measure of the rate of RNA release from the stalled EC and not the rate of translocation of Rho. The differences, if any, in the kinetics will reflect the EC conformational state dependence of Rho action.

Arrested ECs Are Poor Substrates for Rho—Elongation kinetics through the termination zone of the *trp t'* terminator (Fig. 1*A*) revealed a long pause site at +124, which indicates that a stalled EC at this point may backtrack significantly. We stalled the EC at this position, and for comparison, we also stalled the EC at position +161 (Fig. 2*A*). Significant pausing of the EC was not observed at position +161 during the elongation process (Fig. 1*A*). The backtracking potential of the stalled EC was assayed by measuring GreB-induced cleavage of the RNA by the EC. The stalled EC at position +124 was found to be sensitive to GreB-mediated cleavage and could only elongate from this

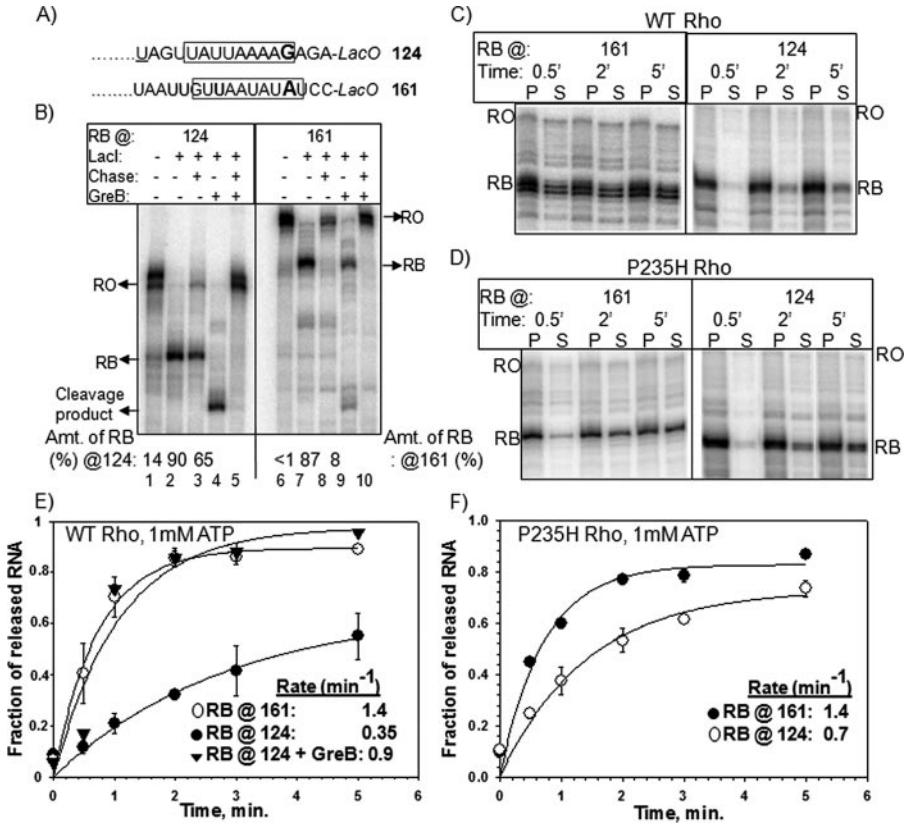

FIGURE 2. **Arrested stalled ECs are poor substrates of Rho.** *A,* RNA sequences of the two templates used to make the stalled elongation complexes at +124 and at +161 positions. The sequences of RNA present in the RNA:DNA hybrid at these positions are shown in the *box* with the 3′ nucleotide highlighted. *B,* autoradiogram showing the positions of the stalled complexes (*RB*), run-off products (*RO*) and GreB-mediated cleavage products under different conditions. *Lanes 3* and *8*, RB was first made and then chased by adding IPTG and NTPs. *Lanes 5* and *10*, cleavage was first induced by GreB, and the cleaved products were then chased with IPTG and NTPs. Fraction of chased complexes were calculated from the band intensities of different products as (RB)/(RB + RO). Autoradiograms showing the time course of RNA release from the stalled elongation complexes at positions +124 and +161 position in the presence of WT (*C*) and P235H (*D*) Rho. *S* (half of the supernatant) and *P* (half of the supernatant + pellet) denote the amount of released RNA and total RNA, respectively. Representative time points are indicated. The plots of fraction of released RNA were plotted against time for WT (*E*) and P235H Rho (*F*). The *curves* were fitted to an exponential rise equation, and rates of RNA release, stated in the *inset* of each panel, were calculated as described under "Experimental Procedures."

position in the presence of GreB (Fig. 2*B*). From the size of the cleavage product, we estimated that the EC at position +124 was backtracked by 8–9 nucleotides. This suggests that the stalled EC at +124 was arrested and irreversibly backtracked. On the other hand, stalled EC at +161 was readily elongated in the absence of GreB and was not significantly sensitive to GreB, which is indicative of its catalytic competence (Fig. 2*B*).

We then followed the time course of RNA release from these two ECs in the presence of either WT or P235H Rho and 1 mM ATP (Fig. 2, *C–F*). Rho released the RNA from the catalytically active stalled EC at position +161 with a high rate and efficiency, whereas the rate of RNA release was ~4-fold and the efficiency was ~2-fold less for the arrested stalled EC at position +124 (Fig. 2, *C* and *E*). The rate and efficiency of RNA release were drastically improved when the +124 EC was activated in the presence of GreB (Fig. 2*E*). A similar improvement was also observed in the presence of a mutant Rho, P235H, which has a higher rate of ATP hydrolysis (42) (Table 2; Fig. 2, *D* and *F*). These results indicate that irreversibly backtracked ECs are a poor substrate for Rho, and a higher rate of ATP hydrolysis is required to dislodge them.

Reversible Backtracking of EC Does Not Affect Rho-dependent RNA Release—The *ops* pause sequence induces pausing because of reversible backtracking of the EC (33). We analyzed Rho-mediated RNA release from the *ops* pause site introduced within the termination zone of the *trp t′* terminator (Fig. 3*A*). Efficient pausing was observed at the o*ps* pause sequence in this context as was revealed from the elongation kinetics through this sequence (Fig. 3*B*). Also, the introduction of this site in the *trp t′* termination zone did not affect Rho-dependent termination (Fig. 3*B*). ECs stalled at this pause site were sensitive to GreB cleavage but were also efficiently elongated both in the presence and absence of GreB (Fig. 3*B*, *right panel*). This suggested that the stalled EC at the *ops* pause site in the *trp t′* termination zone was reversibly backtracked and was catalytically active.

Next Rho-dependent RNA release from the stalled ECs at *ops* site and at +161 were carried out in the presence of 25 μM ATP as in Fig. 2 (Fig. 3, *C* and *D*). Rho released RNA from the stalled EC at the *ops* site with comparable rate and efficiency as that from position +161. Therefore, Rho can release RNA efficiently from a reversibly backtracked EC which is catalytically active.

Catalytic Inactivation of EC by an RNA Hairpin at the Exit Channel Causes Inefficient Rho-dependent RNA Release—Pausing at the *his* pause sequence is proposed to be mediated by interaction of an RNA hairpin with the flap domain of the β-subunit of RNAP located near the RNA exit channel (33–36). The sequence at the *his* pause site codes for RNA that folds into a hairpin near the exit channel. Hairpin-EC interaction at this site was found to cause catalytic inactivation, most likely by allosterically hindering the movement of the trigger-loop (TL) structural element (44). We tested the effect of this *his* hairpin-modified EC on Rho-mediated RNA release. There were two reasons for choosing this modified EC. (i) We observed in Fig. 2 that catalytically inactive, arrested EC is a poor substrate for Rho. The *his* hairpin-EC interaction also causes catalytic inactivation. However, this inactivation is not because of irreversible backtracking of the EC, but because of altered conformations at the active site (44), which is distinct from the conformation of the EC at position +124 (Fig. 2). (ii) If the interaction of Rho with the EC is required for its action, the likely region of interaction will be the RNA exit channel. The *his* hairpin causes conformational changes in

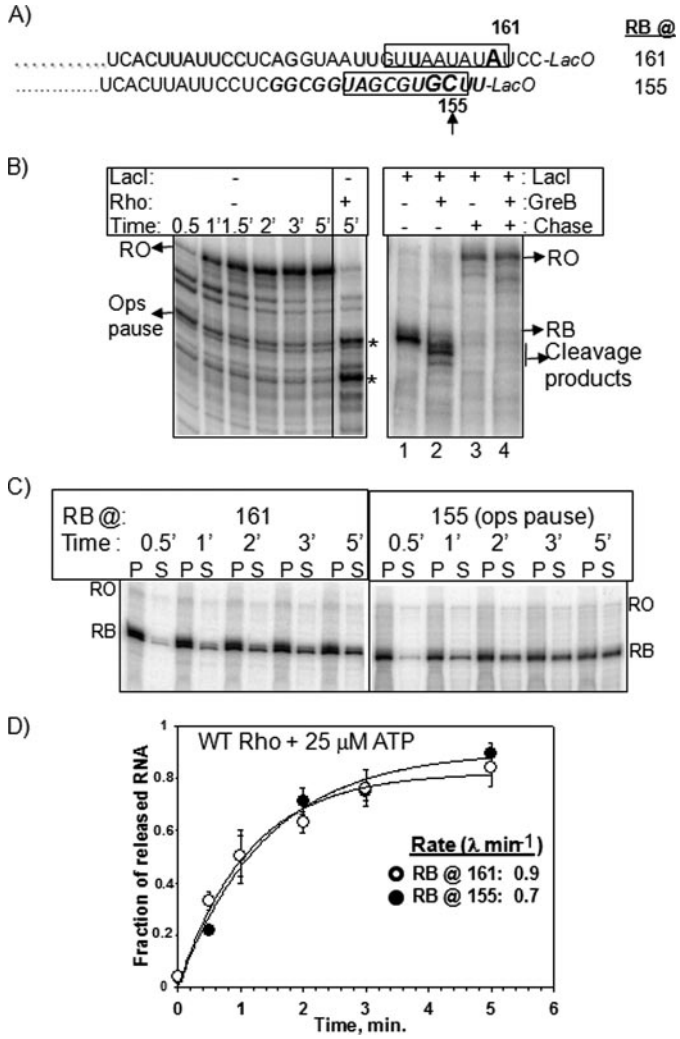

FIGURE 3. **Rho releases RNA efficiently from reversibly backtracked ECs.** *A,* RNA sequence coded from the *ops* pause site (in *boldface italic*) introduced in the *trp t′* termination zone is shown. The 3′-end of the RNA in the RB is at position +151. RNA sequences coded from the *trp t′* terminator zone surrounding position +161 are also shown. Region of RNA present in the RNA:DNA hybrid is *box. B, left panel* shows the autoradiogram of the elongation kinetics through *ops* pause sequence. *Ops* pause site is indicated with an *arrow*. The *right-most lane* of this panel shows Rho-dependent termination from this region with the terminated bands indicated by an *asterisk*. The *right panel* shows the stalled EC (RB) at the *ops* pause site (*lane 1*). This complex is subjected to GreB induced cleavage (*lane 2*) or chased in the presence of IPTG and NTPs either in the absence of GreB (*lane 3*) or after incubating with GreB (*lane 4*). *C,* autoradiogram showing the RNA release time course from stalled ECs at *ops* pause site and position +161 with corresponding plots are shown in *D*. All the notations and calculations of the rates are same as in Fig. 2.

this part of the EC and may also block the approach path of Rho.

We introduced the *his* pause sequence downstream of position +161 in the termination zone of the *trp t′* terminator (Fig. 4*A*). Elongation kinetics, using this construct, revealed an efficient pause 12 nt downstream of the *his* hairpin (+199), which suggested that the *his* pause sequence is functional in this context (Fig. 4*B*). We also tested the hairpin-induced catalytic inactivation of the EC at this pause site, which is indicative of the *his* hairpin-EC interaction at this site. We stalled the EC at +199 by adding *lac* repressor to the reaction and monitored the pyrophosphate cleavage potential of the EC. This is a measure of the catalytic competence of the EC when transcription elongation is blocked by the *lac* repressor (45). We observed very inefficient pyrophosphate cleavage (Fig. 4*C*), indicating that the *his* hairpin in our construct can efficiently cause catalytic inactivation of the EC. Therefore all the properties of *his* hairpin-modified EC were reproduced in our construct, and it can be used to study the effect of this modified EC on Rho-dependent RNA release.

We measured RNA release kinetics by either WT or P235H mutant Rho from the EC stalled at the *his* pause site, in the presence of either low (25 μM) or high (1 mM) concentrations of ATP (Fig. 4, *D–G*). The kinetics of RNA release at the *his* pause site was compared with that obtained from catalytically active EC at position +161. The rate and efficiency of RNA release were found to be reduced significantly at the *his* pause site as compared with that obtained at position +161 (Fig. 4*E*). However, the rate and efficiency of RNA release were improved under the regimen of higher rate of ATP hydrolysis either in the presence of 1 mM ATP (Fig. 4*F*) or P235H Rho (Fig. 4*G*). Analogous to the arrested complex in Fig. 2, Rho can efficiently dislodge the catalytically inactive *his* hairpin-modified EC only when the rate of ATP hydrolysis is higher. A part of the energy from ATP hydrolysis may also be used by Rho to unwind the *his* hairpin.

Effects of the Elongation Inhibitors Tagetitoxin and Streptolydigin on Rho-dependent RNA Release—Results described above strongly suggest that the functional state(s) of the active site of the EC is important for the substrate specificity of Rho. NTP addition cycle during transcription elongation involves the movement of the two important structural elements, the bridge helix (BH) and the trigger loop (TL), located close to the Mg(II)-binding site, and their movement determines the functional state of the active site (46, 47). We hypothesized that any perturbations in the conformational state(s) of these two structural elements will affect Rho-dependent RNA release from the EC.

We modified the EC stalled at position +161 with two antibiotics, streptolydigin (STL) and tagetitoxin (TGT), which bind close to the BH and TL structural elements (Fig. 5*A*) (37, 47) and hinder the movement of these two elements. The STL-bound EC is capable of adding only one nucleotide (38, 39, 48), whereas NTP addition cycle is completely blocked in the TGT-bound form (37). This suggests that in the TGT-bound EC, BH and TL movement may be impermissible, whereas in the STL-bound form these two elements may have limited freedom to move. The modifications of the stalled EC at position +161 with these two antibiotics were at first confirmed from their inability to be elongated efficiently after treating the RBs with IPTG and NTPs (Fig. 5*B*).

We then measured RNA release kinetics by Rho from these modified stalled ECs (Fig. 5, *C–G*). The rate of RNA release by Rho was 2-fold lower when the EC was bound to TGT (Fig. 5, *C* and *E*). This rate, however, improved when P235H mutant instead of WT Rho was used (Fig. 5*F*). Therefore, when internal motion around the active site is impaired, Rho requires a higher rate of ATP hydrolysis to dislodge the EC. Interestingly, Rho was able to dislodge the STL-bound EC efficiently (Fig. 5, *D* and *G*). The STL-bound form offers a little more freedom of movement to the BH and TL elements (38, 39) compared with the

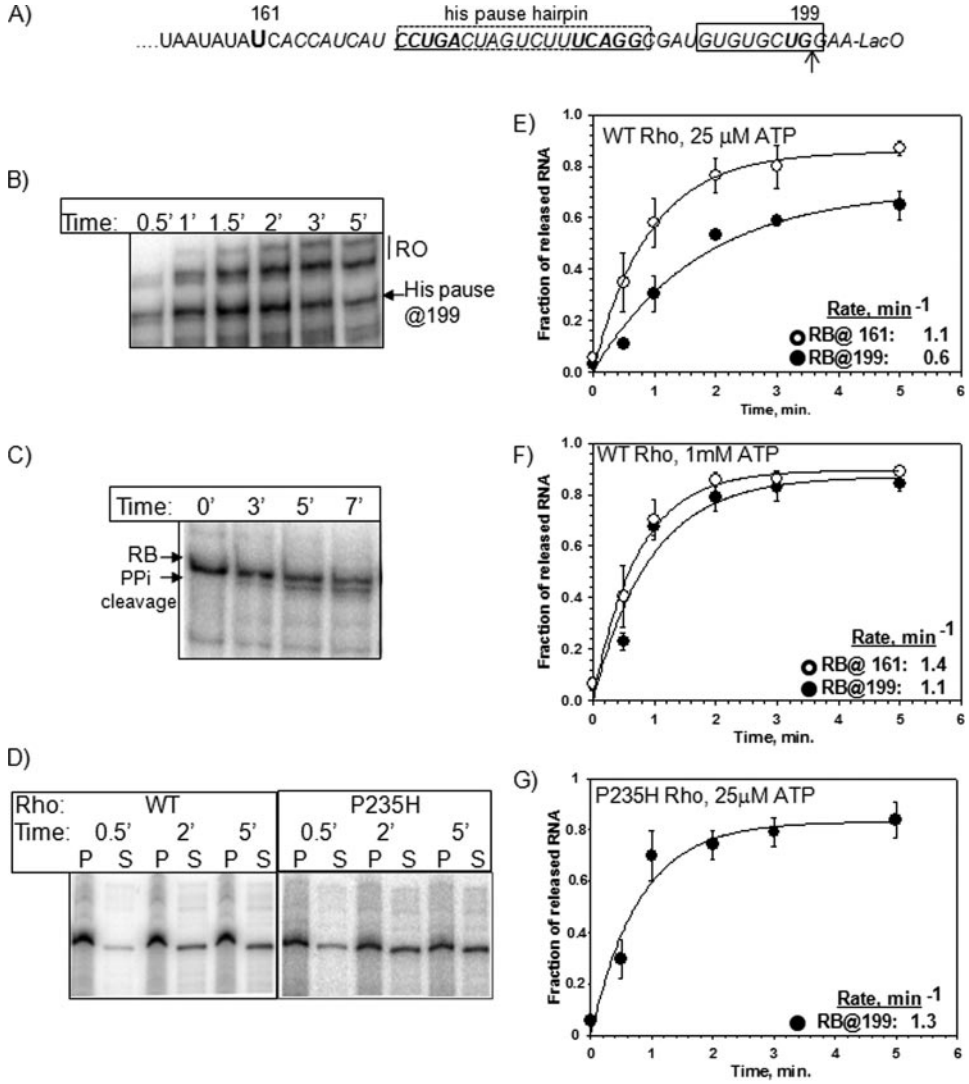

FIGURE 4. **Catalytic inactivation of ECs caused by RNA hairpin at the exit channel affects Rho-dependent RNA release.** *A,* RNA sequence showing the position of the *his* pause sequence downstream of +161 in the *trp t'* terminator zone. *his* pause hairpin-forming sequence is shown in the *dotted box,* and the pause site at +199 is indicated by an *arrow. lac* operator sequence after the pause site is also indicated. Region of RNA present in the RNA:DNA hybrid is marked by a *solid box. B,* autoradiogram showing the elongation kinetics through the *his* pause sequence. *his* pause site and the run-off (*RO*) product are indicated. *C,* autoradiogram showing the pyrophosphorolysis reactions (PP_i cleavage) of the stalled EC (RB) at the *his* pause site in the presence of 1 mM sodium pyrophosphate for the indicated times. *D,* autoradiogram showing the time course of RNA release from stalled EC at the *his* pause site by WT and P235H Rho in the presence of 25 μM ATP. Representative time points are indicated. The plots corresponding to the RNA release kinetics from the RB complexes at the *his* pause site under different conditions are shown in *E–G*. Rates are indicated in the *inset* of each panel. All the calculations and notations are as in Fig. 2.

TGT-bound form (37), which might be sufficient for Rho to exert its action. As the BH/TL movement plays an important role in Rho action, it is likely that hindered TL movement in the *his* hairpin-modified EC (44) may have also affected the efficiency of RNA release by Rho from that complex (Fig. 4).

DISCUSSION

Pausing of the EC in the termination zone of Rho-dependent terminators is required for coupling the transcription elongation and the translocation of Rho (24, 25). ECs can exist in different conformational states at these pause sites (28). Here we present strong evidence that the rate and efficiency of RNA release by Rho are highly influenced by the conformational states of the EC in the termination zone. We showed the following: 1) pausing associated with the termination points is very short lived (Fig. 1); 2) irreversibly backtracked (Fig. 2) and *his* hairpin-modified ECs are poor substrates for Rho (Fig. 4); 3) RNA release by Rho is affected if the free movement of BH/TL structures in the active site of the EC is blocked completely by the inhibitor tagetitoxin (Fig. 5); and 4) increase in the rate of ATP hydrolysis by Rho (Table 2, A and B) is proportional to an increase in the rate of Rho-dependent RNA release from different stalled ECs. A higher rate of ATP hydrolysis by Rho is essential to release RNA efficiently from the catalytically inactive ECs (Figs. 2, 4, and 5). We concluded that the dislodging of the EC by Rho is facilitated only when the RNAP is engaged in active transcription.

It has been proposed that a complex Brownian ratchet motion involving the oscillation of the two structural elements, BL and TL, in the active center governs the nucleotide addition cycle during elongation (46). Structural and biochemical evidence suggests that catalytic inactivation of the ECs, modified either by the *his* hairpin (44) or by the antibiotic TGT (37), is because of blockage of the movement of BL and TL structural elements. The oscillation of these two structural elements is also likely to be hindered when the 3′-end of the RNA occupies the secondary channel in an arrested or irreversibly backtracked complex. We showed here that Rho-dependent RNA release is significantly affected in all these modified ECs, which suggests that conformational flexibility around the active center plays a key role in the process of termination. This suggestion is further supported by the fact that Rho can efficiently release RNA from a reversibly backtracked complex, where presumably the Brownian ratchet motion is not hindered, and from an STL-bound EC where some movement of BH and TL is allowed (38, 39).

What is the role of ATP hydrolysis during Rho-mediated RNA release from the EC? We observed that there is a direct correlation between the rate of ATP hydrolysis by Rho and its efficiency of RNA release from the stalled ECs. ATP hydrolysis by Rho is required for its transcription termination function (40, 41). Although there is no direct evidence, it is believed that the free energy derived from this ATP hydrolysis is used for the translocation as well as the motor action of Rho (43). We spec-

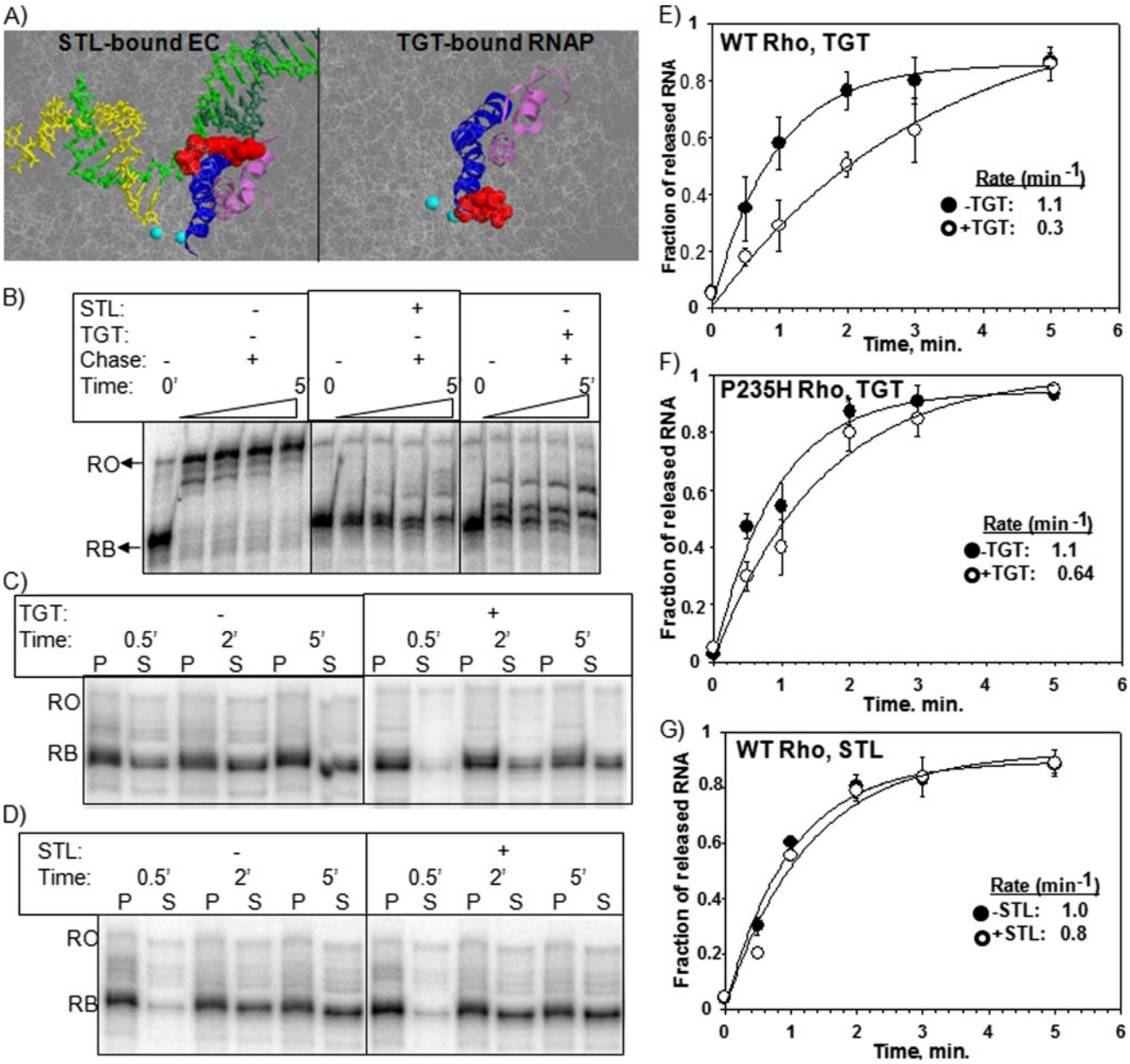

FIGURE 5. **Movement of bridge helix and trigger loop in the active center of the EC is important for Rho action.** *A,* view of the nucleic acid framework in the structure of elongation complex bound with STL is shown in the *left panel*. A similar view of TGT-bound RNA polymerase is shown in the *right panel*. The images were prepared from the structural coordinates available from Protein Data Bank (2PPB (48) and 2BE5, (37)) using RASMOL. The BH and TL structures in both figures are highlighted in *blue* and *pink*, respectively. The locations of antibiotics and Mg(II) in both figures are shown as *red* and *cyan spheres*, respectively. The rest of the RNAP structures are shown in a *gray background. B,* autoradiograms showing the chasing kinetics of the stalled ECs (RB) at position +161 modified with the STL and TGT. RB complexes were first incubated with respective antibiotics for 5 min and were then chased with IPTG and NTPs. *Triangles* indicate the increasing time points ranging between 0 and 5 min. Autoradiograms showing the representative time points of the time course of RNA release from the stalled elongation complexes at position +161 modified either with tagetitoxin (*C*) or with streptolydigin (*D*). The concentration of ATP was 25 μM. Corresponding plots for RNA release kinetics under different conditions are shown in *E–G*. Calculations of the rates of RNA release were performed as in Fig. 2.

ulate that increase in the rate of ATP hydrolysis will also increase the translocation speed of Rho and will impart more kinetic energy to this molecular motor. This kinetic energy will be used by Rho to exert force on the elongation complex to dislodge it. A higher rate of ATP hydrolysis will ultimately be translated into a higher force that will enable Rho to act upon the poor substrates. However, this hypothesis can only be tested by a direct measurement of the force exerted by Rho using single molecule measurements. Alternatively, it may be possible that each ATP hydrolysis step by Rho is directly linked to each step of RNA release and later may involve successive steps of pulling the RNA out of the EC or pushing the EC forward. In this model, it is likely that under the regimen of a higher rate of ATP hydrolysis, the steps involved in RNA release will become faster and will outperform the NTP addition cycle of the EC. However, linking ATP hydrolysis to the steps of RNA release will also involve the utilization of the energy obtained from the hydrolysis reactions.

Why does Rho prefer catalytically competent ECs for termination? At the peak of the elongation process, the rapid Brown-

ian ratchet motion at the active center of the EC will cause breakage and formation of multiple noncovalent interactions, which may confer overall instability to the EC as compared with when it is trapped in a static conformation incapable of pursuing nucleotide addition cycles. According to our speculation, less force generated by the lower rate of ATP hydrolysis by Rho is sufficient to dissociate these relatively less stable catalytically active ECs, whereas an enhanced rate of ATP hydrolysis is required to act on the more stable inactive complexes. We propose that Rho employs a "brute force" mechanism to dislodge the EC, in which the force generated by the ATP hydrolysis sets off its molecular motor action, which in turn displaces the EC. This proposal is consistent with the recent observation that translocation of Rho can break a strong biotin-streptavidin interaction present at the end of an RNA template (49).

Acknowledgments—We thank Dr. Rashna Bhandari and other laboratory members for critically reading the manuscript, Jineta Banerjee for preparing the P235H Rho, and Prof. Nobuo Shimamoto for insightful comments.

REFERENCES

1. Wilson, K. S., and von Hippel, P. H. (1994) *J. Mol. Biol.* **244,** 36–51
2. Mooney, R. A., Artsimovitch, I., and Landick, R. (1998) *J. Bacteriol.* **180,** 3265–3275
3. Yarnell, W. S., and Roberts, J. W. (1999) *Science* **284,** 611–615
4. Richardson, J. P. (1993) *Crit. Rev. Biochem. Mol. Biol.* **28,** 1–30
5. Uptain, S. M., Kane, C. M., and Chamberlin, M. J. (1997) *Annu. Rev. Biochem.* **66,** 117–172
6. Richardson, J. P. (2003) *Cell* **114,** 157–159
7. Richardson, J. P. (2002) *Biochim. Biophys. Acta* **1577,** 251–260
8. Banerjee, S., Chalissery, J., Bandey, I., and Sen, R. (2006) *J. Microbiol.* **44,** 11–22
9. Modrak, D., and Richardson, J. P. (1994) *Biochemistry* **33,** 8292–8299
10. Wei, R. R., and Richardson, J. P. (2001) *J. Biol. Chem.* **276,** 28380–28387
11. Burgess, B. R., and Richardson, J. P. (2001) *J. Biol. Chem.* **276,** 4182–4189
12. Wei, R. R., and Richardson, J. P. (2001) *J. Mol. Biol.* **314,** 1007–1015
13. Xu, Y., Kohn, H., and Widger, W. R. (2002) *J. Biol. Chem.* **277,** 30023–30030
14. Miwa, Y., Horiguchi, T., and Shigesada, K. (1995) *J. Mol. Biol.* **254,** 815–837
15. Skordalakes, E., and Berger, J. M. (2003) *Cell* **114,** 135–146
16. Skordalakes, E., and Berger, J. M. (2006) *Cell* **127,** 553–564
17. Alifano, P., Rivellini, F., Limauro, D., Bruni, C. B., and Carlomagno, M. S. (1991) *Cell* **64,** 553–563
18. Morgan, W. D., Bear, D. G., Litchman, B. L., and von Hippel, P. H. (1985) *Nucleic Acids Res.* **13,** 3739–3754
19. Bear, D. G., Hicks, P. S., Escudero, K. W., Andrews, C. L., McSwiggen, J. A., and von Hippel, P. H. (1988) *J. Mol. Biol.* **199,** 623–635
20. Ciampi, M. S. (2006) *Microbiology* **152,** 2525–2528
21. Morgan, W. D., Bear, D. G., and von Hippel, P. H. (1983) *J. Biol. Chem.* **258,** 9553–9564
22. Chen, C. Y., and Richardson, J. P. (1987) *J. Biol. Chem.* **262,** 11292–11299
23. Zalatan, F., Galloway-Salvo, J., and Platt, T. (1993) *J. Biol. Chem.* **268,** 17051–17056
24. Richardson, L. V., and Richardson, J. P. (1996) *J. Biol. Chem.* **271,** 21597–21603
25. Farnham, P. J., Greenblatt, J., and Platt, J. (1982) *Cell* **29,** 945–951
26. Laus, L. F., Roberts, J. W., and Wu, R. (1983) *J. Biol. Chem.* **258,** 9391–9397
27. Kassavetis, G. A., and Chamberlin, M. J. (1981) *J. Biol. Chem.* **256,** 2777–2786
28. Landick, R. (2006) *Biochem. Soc. Trans.* **34,** 1062–1066
29. Nudler, E., and Gottesman, M. E. (2002) *Genes Cells* **7,** 755–768
30. Cheeran, A., Babu Suganthan, R., Swapna, G., Bandey, I., Achary, M. S., Nagarajaram, H. A., and Sen, R. (2005). *J. Mol. Biol.* **352,** 28–43
31. Chalissery, J., Banerjee, S., Bandey, I., and Sen, R. (2007) *J. Mol. Biol.* **371,** 855–872
32. King, R. A., Sen, R., and Weisberg, R. A. (2003) *Methods Enzymol.* **371,** 207–218
33. Artsimovitch, I., and Landick, R. (2000) *Proc. Natl. Acad. Sci. U. S. A.* **97,** 7090–7095
34. Chan, C. L., Wang, D., and Landick, R. (1997) *J. Mol. Biol.* **268,** 54–68
35. Toulokhonov, I., Artsimovitch, I., and Landick, R. (2001) *Science* **292,** 730–733
36. Toulokhonov, I., and Landick, R. (2003) *Mol. Cell* **12,** 1125–1136
37. Vassylyev, D. G., Svetlov, V., Vassylyeva, M. N., Perederina, A., Igarashi, N., Matsugaki, N., Wakatsuki, S., and Artsimovitch, I. (2005) *Nat. Struct. Mol. Biol.* **12,** 1086–1093
38. Temiakov, D., Zenkin, N., Vassylyeva, M. N., Perederina, A., Tahirov, T. H., Kashkina, E., Savkina, M., Zorov, S., Nikiforov, V., Igarashi, N., Matsugaki, N., Wakatsuki, S., Severinov, K., and Vassylyev, D. G. (2005). *Mol. Cell* **19,** 655–666
39. Tuske, S., Sarafianos, S. G., Wang, X., Hudson, B., Sineva, E., Mukhopadhyay, J., Birktoft, J. J., Leroy, O., Ismail, S., Clark, A. D., Jr., Dharia, C., Napoli, A., Laptenko, O., Lee, J., Borukhov, S., Ebright, R. H., and Arnold, E. (2005) *Cell* **122,** 541–552
40. Shigesada, K., and Wu, C. W. (1980) *Nucleic Acids Res.* **8,** 3355–3369
41. Howard, B. H., and de Crombrugghe, B. (1976) *J. Biol. Chem.* **251,** 2520–2524
42. Periera, S., and Platt, T. (1995) *J. Mol. Biol.* **251,** 36–40
43. Brenan, C. A., Dombrowski, A. J., and Platt, T. (1987) *Cell* **48,** 945–952
44. Toulokhonov, I., Zhang, J., Palanghat, M., and Landick, R. (2007) *Mol. Cell* **27,** 406–419
45. Sosunov, V., Sosunova, E., Mustaev, A., Bass, I., Nikiforov, V., and Goldfarb, A. (2003) *EMBO J.* **22,** 2234–2244
46. Bar-Nahum, G., Epshtein, V., Ruckenstein, A. E., Rafikov, R., Mustaev, A., and Nudler, E. (2005) *Cell* **120,** 183–193
47. Vassylyev, D. G., Vassylyeva, M. N., Perederina, A., Tahirov, T. H., and Artsimovitch, I. (2007) *Nature* **448,** 157–162
48. Vassylyev, D. G., Vassylyeva, M. N., Zhang, J., Palangat, M., Artsimovitch, I., and Landick, R. (2007) *Nature* **448,** 163–168
49. Schwartz, A., Margeat, E., Rahmouni, A. R., and Boudvillain, M. (2007) *J. Biol. Chem.* **282,** 31469–31476
50. Pani, B., Banerjee, S., Chalissery, J., Abishek, M., Loganathan, R. M., Suganathan, R. B., and Sen, R. (2006) *J. Biol. Chem.* **281,** 26491–26500

Transcription Termination Factor Rho Prefers Catalytically Active Elongation Complexes for Releasing RNA

Dipak Dutta, Jisha Chalissery and Ranjan Sen

J. Biol. Chem. 2008, 283:20243-20251.
doi: 10.1074/jbc.M801926200 originally published online May 15, 2008
